Environment and Climate Protection (2022)
Clausius Scientific Press, Canada

DOI: 10.23977/envcp.2022.010103
ISSN 2523-6504 Vol. 1 Num. 1

Preliminary Analysis of Multi-Typhoon Influence on Hainan Province and Its Circulation Background in Autumn 2020

Chenxiao Shi[1,2], Chunxiang Shi[3,*], Tao Zhang[3], Jianhua Du[1,2], Honghui Zheng[1,2], Zhenli Chen[1,2]

[1]Hainan Province Meteorological Information Center, Haikou, Hainan, China
[2]Key Laboratory of South China Sea Meteorological Disaster Prevention and Mitigation of Hainan Provinces, Haikou, Hainan, China
[3]National Meteorological Information Center, Beijing, China
[*]Corresponding author

Keywords: Multi-typhoon, circulation background, subtropical high pressure, cold air, SST pleion, OLR negative anomaly area

Abstract: In order to understand some factors that many typhoons will affect the climate background and atmosphere and ocean of Hainan Province in the autumn of 2020, this paper makes a preliminary analysis of the characteristics and circulation background of many typhoons in the autumn of 2020 by using multi-source merged products, China's first generation reanalysis products (CRA-40), satellite data and ground observation data. During the period from October to November in 2021, the location of the subtropical high is east-north compared with previous years, and its intensity was weak. As a result, under the guidance of the southeasterly airstream at the edge of the subtropical high, eight typhoons converged in Hainan Province and western Guangdong, and the vertical velocity over them was basically negative, resulting in a continuous and strong wind and rain process in this area. From October to November, positive SST anomalies near the equatorial western Pacific and the South China Sea provide a steady stream of energy for typhoons in the South China Sea and the western Pacific Ocean, and negative OLR anomalies cause large-scale strong convective activities. Combined with the actual observation, it can be seen that the area of strong convective activity is mainly concentrated in the areas of 5-20 ℃N and 110-150 ℃E, which is the place where the sea temperature is abnormal in 2020 and the place where typhoons originated.

1. Introduction

Typhoons affect coastal areas mainly through strong winds, heavy rainfall and tides, which brings great influence to the production and life of coastal areas. In 2005, hurricane Katrina and Rita attacked coastal area of the USA, which caused deaths of about 1400 people and economical loss of $400 billion in the city of New Orleans and destroyed more than 110 platforms in the Gulf of Mexico[1]. In 2013, the super typhoon Haiyan landed and crossed the central Philippines, killing

more than 6,000 people and missing about 1,800 people, causing major damage to infrastructure, property, power and communication[2]. In 2017, Hurricane Harvey landed on the southern coast of Texas, USA, causing a rare flood disaster in Houston, the capital of Texas, which killed 44 people and affected 1.3 million people, and hit the US energy industry hard[3]. China is one of the countries in the world which is most severely affected by typhoons, and its whole coastline can be affected by typhoons[4-11]. Typhoon “Morakot” in 2009 caused a major disaster in southern Taiwan Province. Besides economic losses, about 700 people were killed or missing[12-14]. Typhoon “Fete” in 2013 caused extreme precipitation and storm surge along the north-central coast of Zhejiang Province, which caused Yuyao and other cities to be flooded for more than a week[15]. In 2014, the typhoon “Rammasun” landed in Hainan Island with super typhoon level, causing 3,258,300 people to be affected and 25 people to die, and the direct economic loss reached 11.952 billion yuan[16]. In 2018, the super typhoon “Mangosteen” landed in Guangdong, causing 458 villages and towns to be affected, 4 people died and the direct economic loss was 4.229 billion yuan[17]. In 2019, the super typhoon "Lichima" landed in Wenling, Zhejiang Province, and then went northward, causing serious impacts on the eastern coast and inland areas of China, resulting in 71 deaths or missing persons and direct economic losses exceeding 53 billion yuan[18].

The area studied in this paper is just located in the coastal area of South China. The main generation areas of typhoons in China are located in the South China Sea and the western Pacific Ocean. In summer, there is often an east-west tropical convergence zone cloud belt in the South China Sea and the western Pacific Ocean, in which the cloud masses often correspond to the vortices or disturbances in the convergence zone, followed by continuous development, eventually forming a situation where typhoons appear one after the other or multiple typhoons coexist[19-22]. It should be noted here that "multiple typhoons" in this paper means that typhoons are generated one after another and continuously affect a certain region or province in a certain period of time in a certain year, but not a certain region or province for many years. Xu Jinjing et al.[23] analyzed the circulation situation and SST changes in Fujian and Peng Benxian[24] in southeast China during May-October 1999, Guangxi in South China in October 1983 and Liu Na et al.[25] analyzed the circulation situation and SST change in Jilin in Northeast China from July to August, 2018, and pointed out that the frequent influence of many typhoons in that year was mainly caused by abnormal SST and subtropical high position.

As the only tropical island province in China, Hainan Province is composed of numerous islands and the vast South China Sea. Because of its special geographical location, it is affected by typhoons every year. According to the statistics of the Hainan Climate Center on typhoons that landed or affected Hainan Province since 1949, there were 149 typhoons that landed in Hainan Island from 1949 to 2014, among which typhoon Maqi landed in Boao Town, Qionghai, Hainan in 1973, causing 926 deaths, 1,690 serious injuries and 4,470 minor injuries in Hainan, which is the typhoon with the largest death toll in Hainan since 1949. In 2014, the typhoon "Rammasun" caused disasters in 216 towns and villages in 18 cities and counties in Hainan Province, with 3,258,300 people affected and 23,163 houses collapsed, with a total direct economic loss of 11.952 billion yuan, which was the heaviest typhoon in Hainan Province since 1949. However, in the autumn of 2020, typhoons were constantly generated in the western Pacific Ocean or the South China Sea, showing a "ebb and flow" state, and even at the end of October and the beginning of November, the situation of double typhoons coexisted, which was different from the historical average record. Then, we need to compare the characteristics, circulation background and differences between SST and typhoons in previous years, which continuously directly or indirectly affect Hainan Province in October-November, 2020.In addition, by summarizing the above scholars' research and analysis, it is found that there are few studies on the continuous influence of multiple typhoons on a certain area in China, the analysis is limited to the analysis of circulation situation and sea temperature, and

the OLR is not analyzed. In this paper, it is considered that the reason for adding OLR analysis is that global warming will affect the amount of cloud cover, and then affect the circulation of water vapor, which can reflect the anomalies caused by multiple typhoons from the side.

2. Data Information Description

The main analytical data used in this paper are multi-source merged data of different meteorological elements independently developed by China, China's first generation reanalysis data (CRA-40) and satellite data, which is quite different from the American data used by many scholars when studying typhoons.

2.1. Multi-Source Merged Data

2.1.1. CMA Multi-Source Merged Precipitation Analysis System (CMPAS-V2.1)

CMPAS is a ground-satellite-radar fusion precipitation analysis product for China (CMPAS-V2.1), which is a multi-source precipitation fusion analysis product with high spatial and temporal resolution in China. This data product is a three-source precipitation fusion product with a resolution of 0.01 °. It adds the DS method to form the "PDF+BMA+DS+OI" on the basis of the original three-source fused hourly precipitation product with 0.05 ° resolution. CMPAS-V2.1 is a fused precipitation analysis product providing both 0.05 ° and 0.01 ° spatial resolution hour-by-hour precipitation products[26-31]. In the present paper, a three-source fused precipitation analysis product with a spatial resolution of 0.01 °and a temporal resolution of 1 hour is selected. In addition, the CMPAS China day-by-day precipitation live fusion analysis product is accumulated from the CMPAS China hour-by-hour precipitation live fusion analysis products.

2.1.2. Centigrade of Global Ocean Day Analysis System (CODAS)

The CODAS, Centigrade of global ocean day analysis system, which is a fusion analysis product which covers the global area with a spatial resolution of 0.25 °×0.25 ° with equal latitude and longitude grids. The data collection is created by using multiple sources of satellite, ship, buoy and other observations and using key technologies such as bias revision and fusion analysis, and the RMSE of the fusion product is less than 0.5K (Kelvin).The data product generates the SST fusion product of the previous day (08-08 BST) at 10:00 BST daily.

2.2 Global Chinese Reanalysis (CRA-40) Dataset

CRA-40 is a global reanalysis dataset developed by the National Meteorological Information Center (NMIC) of the China Meteorological Administration (CMA), covering the period of 1979–2018. It is China’s first generation of global atmospheric reanalysis product released recently. It employs the NCEP GFS/GSI (Global Forecast System/Gridpoint Statistical Interpolation) 3D-Var system with 64 vertical levels. The horizontal resolution is 34 km (T574)[32-35].

2.3 Satallite Data

FY-3D MERSI-II Monthly Emission of long-wave radiations products are monthly averaged ones which are generated on the basis of MERSI-II Daily Emission of long-wave radiations products, which has a spatial resolution of 0.5 ° × 0.5 °and equal latitude and longitude projection.

3. General Situation of Multi-Typhoon Profile and Its Impact Features

3.1 Overview of Typhoons in October and November

By the end of 2020, there were 23 typhoons generated in the northwest Pacific Ocean and the South China Sea waters, which was 2.5 less than the previous year, and which 5 typhoons made landfall in China, which was 2.2 less than previous years[36]. In July, there were no typhoons generated or landed in the South China Sea and the western Pacific; from late August to early September, there were a total of three typhoons affecting the northeast of China. 8 typhoons affected or landed in China in October-November, among which only one typhoon landed in China. Among them, "LINFA", "NANGKA", "ETAU", three typhoons generated in the South China Sea, while the rest of the typhoons are generated in the western Pacific Ocean, that is, east of the Philippines on the ocean. "SAUDEL" and "MOLAVE" strengthened to typhoon level after entering the South China Sea, and "VAMCO" strengthened to strong typhoon level once it entered the South China Sea. The "GONI" and "ATSANI" were generated successively, which generated the situation of double typhoons coexisted. Typhoons affecting or landing in China in October-November 2020 are summarized in Figure 1 and Table 1.

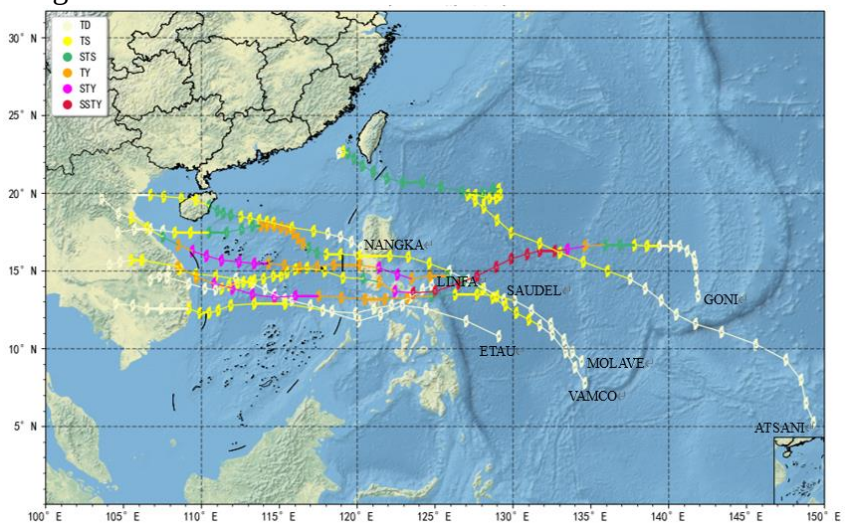

Figure 1: multi-typhoon path map in October-November 2020

Table 1: Overview of typhoons affecting or landing in China in October-November 2020

No.	Name	Typhoon Generation			Typhoon Intensity		Stopping time
		Time (UTC)	Lon(℉)	Lat (℃)	Pres. (hpa)	WS (m/s)	(UTC)
2015	LINFA	Oct. 07th 06:00	124.8	14.1	995	20	Oct. 12th 00:00
2016	NANGKA	Oct. 11th 00:00	120.2	16.5	988	25	Oct. 14th 12:00
2017	SAUDEL	Oct. 19th 00:00	129.4	13.2	965	38	Oct. 26th 06:00
2018	MOLAVE	Oct. 23th 00:00	134.4	9.2	950	48	Oct. 29th 06:00
2019	GONI	Oct. 26th 12:00	141.9	13.4	900	70	Nov. 06th 06:00
2020	ATSANI	Oct. 29th 00:00	149.3	5.3	988	25	Nov. 07th 12:00
2021	ETAU	Nov. 07th 00:00	129.1	10.8	985	25	Nov. 11th 06:00
2022	VAMCO	Nov. 08th 00:00	134.6	7.8	945	48	Nov. 16th 00:00

3.2 The Impact of Multiple Typhoons on Hainan Province

Eight typhoons were generated From October to November, 5 of which brought strong winds

and heavy rainfall to Hainan Province directly or indirectly, resulting in certain economic losses. Let's take Typhoon "NANGKA", Typhoon "SAUDEL" and Typhoon "VAMCO" as examples.

While Typhoon "LINFA" (2015) was about to fade away on the 11th, Typhoon "NANGKA" (2016) was gradually generated offshore to the west of the Philippines at 14:00 on the 11th, gradually increasing in intensity and moving in a westerly-northerly direction. NANGKA strengthened to strong tropical storm level at 11:00 on the 13th, when the typhoon center is about 143 kilometers eastward from Wanning City, Hainan Province, in the northern sea of the South China Sea, where the maximum wind near the center of 10 (25 m/s). At about 19:20 on the evening of the 13th, NANGKA landed in Qionghai City, Hainan Province at the level of a strong tropical storm. After that, the typhoon decreased in intensity to a tropical storm and quickly crossed Hainan Island. According to the statistics of the Provincial Third Defense Office, when typhoon "NANGKA" landed on Hainan Island that night, a cargo ship capsized and sank near the Qiongzhou Strait in Hainan, causing two people on board to be killed and three people missing. In addition, typhoon "NANGKA" caused farmland flooded at Baoluo town, Wenchang City and 859.95 mu of crops were destroyed, with direct economic losses of about 1.302 million yuan. Qiongzhong County, 45 places of provincial and national roads were collapse, the village roads were damaged and 24 places of production right-of-way were collapsed, which caused a direct economic loss of about 1.54 million yuan. Qiongzhong County, 45 places of provincial and national roads were collapse, the village roads were damaged and 24 places of production right-of-way were collapsed, which caused a direct economic loss of about 1.54 million yuan. It made landfall again off the coast of Thanh Hoa, Vietnam at 18:20 on the 14th. As the intensity weakened again, the Central Weather Station stopped numbering it at 20:00 on the 14th.

As can be seen from the spatial and temporal distribution of precipitation map (Figure 2a and b), Hainan had a strong rainfall process from 05:00 on the 13th to 23:00 on the 14th.In particular, the northern and eastern regions of Hainan is the province's rainfall large value area. According to the measured data, only on the 14th, the cumulative rainfall in Haikou City reached 101.0 mm, followed by 94.1 mm in Dingan County, while other cities and counties including Tunchang County, Qionghai City, Wenchang City and Baoting County all had cumulative rainfall of 65.0 mm or more. Combined with CMPAS live precipitation distribution (Figure 2c~d) at 20-21 on the 13th and 14 on the 14th , we can see that the precipitation distribution of typhoon "NANGKA", which showed that typhoon rainfall was in the large value area at the junction of Dingan County , Tunchang County and Qionghai City at 21:00 on the 13th . With the landfall of typhoon "NANGKA ", the typhoon periphery and cold air interacted with each other, although the typhoon westbound into the Gulf of Tonkin, but in the 14th Hainan Province still have rainfall process, of which the eastern and northern for the rainfall of the large value area.

October 19, No.2017 typhoon "SAUDEL" generated in the ocean to the east of Philippines, and then moved to the west-northwest. The intensity gradually increased. It entered the waters of the South China Sea at the level of a tropical storm on the 21st, moving faster and stronger, strengthening to typhoon level at 14:00 on the 22nd, and continued to move in the west-northwest direction. At 08:00 on the 24th, it weakened to a strong tropical storm, moving westward and brushing the island of Hainan all the way. At 11:00 on the 25th, it continued to weaken to a tropical storm, and at 02:00 on the 26th, the Central Weather Station stopped numbering it. Affected by "SAUDEL" and cold air together, Hainan Province, after experiencing the impact of "NANGKA", once again experienced high winds and heavy precipitation process.

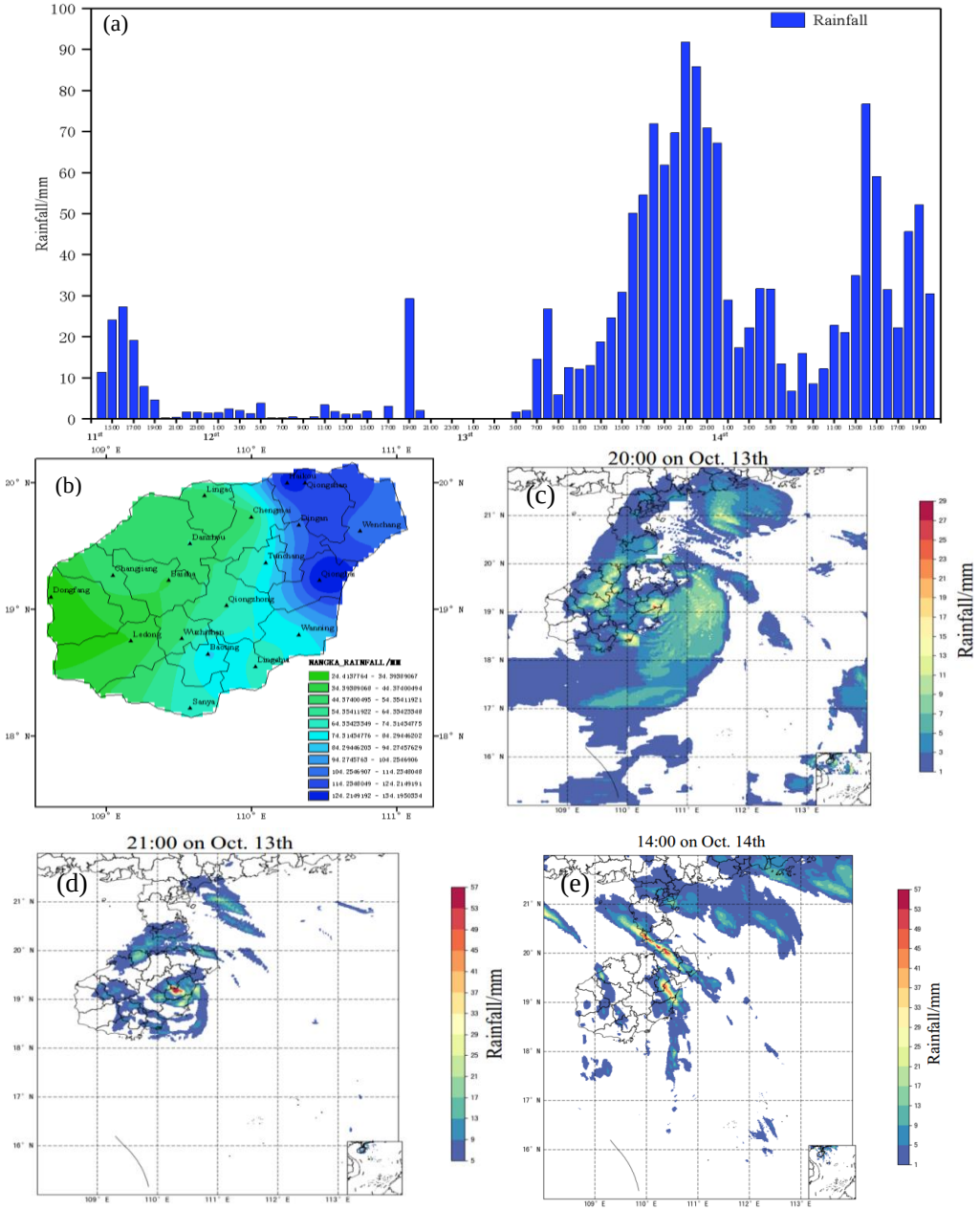

Figure 2: Spatial and temporal distribution of rainstorm measured by Typhoon NANGKA (a, b) and the CMPAS live precipitation distribution maps at 20-21 hours on the 13th (c, d) and 14 hours on the 14th (e)

According to the statistics of the Provincial Third Defense Office, in Coconut Grove Town, Lingshui County, 23.3 hectares of rice was damaged; in Yingzhou Town, 120 hectares of rice was damaged; in Wen Luo Town, 1.66 hectares of rice was damaged; in Timon Town, 9.66 hectares of rice was damaged; in Benhao Town, 8 hectares of rice was damaged; in Long Guang Town, 23 hectares of rice was damaged.

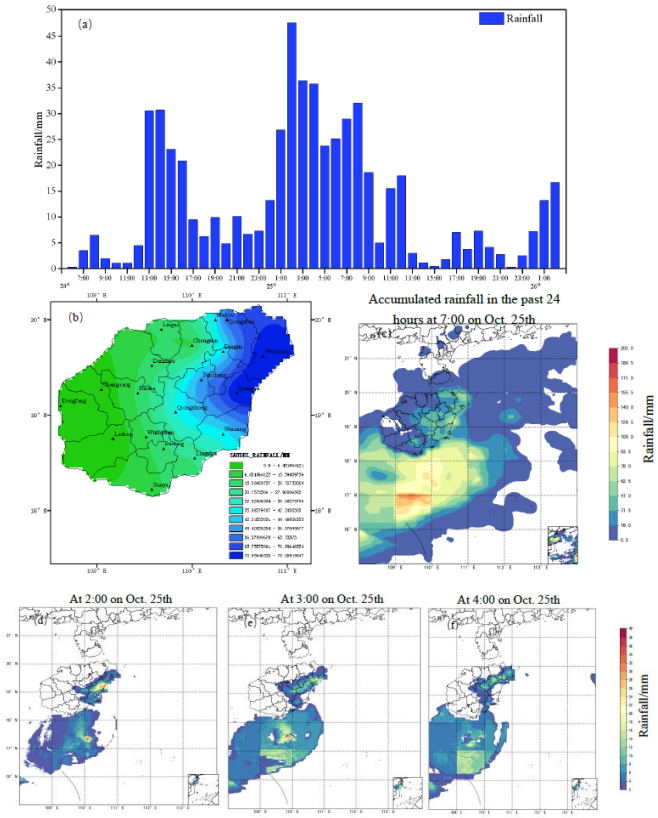

Figure 3: Spatial and temporal distribution of rainstorm measured by Typhoon "SAUDEL" (a, b) and the accumulated rainfall in the past 24 hours at 07:00 on October 25 (c) and 02:00-04:00 on October 25 (d~f)

From the spatial and temporal distribution of precipitation map can be seen (Figure 3a, b) that Hainan Province has a strong precipitation process from 07:00 on the 24th, and the accumulated rainfall reached the maximum by 07:00 on the 25th. Among them, the accumulation of rainfall in Qionghai is 77.6 mm, which is followed by the accumulation of rainfall in Wenchang of 60.9 mm. The northwestern part of Hainan Island had less rainfall, among which Dongfang City had no precipitation, Changjiang County's accumulation of rainfall was only 0.6 mm, and Ledong County's accumulation of precipitation was only 0.7 mm. It can be seen that the rainfall process is relatively less in comparison with Typhoon "NANGKA", but the rainfall value area is still in the northeastern part of Hainan Island. Combined with the distribution of the past 24 hours of live rainfall at 07:00 on the 25th (Figure 3c), when the typhoon "SAUDEL" grazed Hainan Island, there was also strong rainfall at sea. From the real-time live rainfall distribution map at 02:00-04:00 on the 25th (Figure 3d~f), the fall zone of heavy precipitation on land appeared successively in the territory of Qionghai City and Wenchang City, and the rain band moved westward, which is generally consistent with the actual observation results.

Typhoon "VAMCO"(2022) generated at 14:00 in November 09 on the ocean surface to the east of the Philippines, which is also the last typhoon affecting Hainan Province in 2020. After the generation of the typhoon to the west-northwest direction, the strength gradually increased, and it strengthened to a strong tropical storm level at 17:00 on the 10th. Before landing in the Philippines, it has strengthened to a strong typhoon level. Influenced by the mountain range, "VAMCO" weakened to typhoon level after landing in the Philippines. At 19:00 on the 13th, it strengthened again to become a strong typhoon and weakened to typhoon level before landing in Vietnam. As the center of the typhoon got closer to Vietnam, "VAMCO" weakened again to strong tropical storm

level. The intensity weakened again to a hot spot low pressure after landing in Vietnam, and perished at 17:00 on November 15. It took a total of 7 days for the typhoon to experience from the generation to the demise. Although it did not make landfall in Hainan Province, it also brought stronger gale and rainfall process to Hainan Province.

It can be seen from the spatial and temporal distribution of precipitation map (Figure 4a~b) that there was a strong rainfall process in Hainan Province from 13:00 on the 12th. Acknowledging that the typhoon kept moving westward from the east, the first to be affected were Yongxing Island and Coral Island in Sansha City. On the basis of the actual measured values, the daily rainfall on the two islands reached 113.4 mm and 158.2 mm respectively on the 14th, and the great wind speed reached 22.8 m/s and 29.6 m/s respectively. By the 15th, the daily rainfall in Ledong County reached 158.2 mm, and the daily rainfall in Qionghai City and Tunchang County both reached more than 100.0 mm. Apart from the northern areas where there was less precipitation, the precipitation in other areas was essentially 46.91 mm or more. In conjunction with the distribution of accumulated live rainfall from 00:00 on the 14th to 00:00 on the 16th (Figure 4c), the main occurrence areas of heavy precipitation are located in the central-eastern part of Hainan Island and the junction of Ledong County, Sanya City, Baoting County and Wuzhishan City, which is basically consistent with the spatial distribution of the measured values.

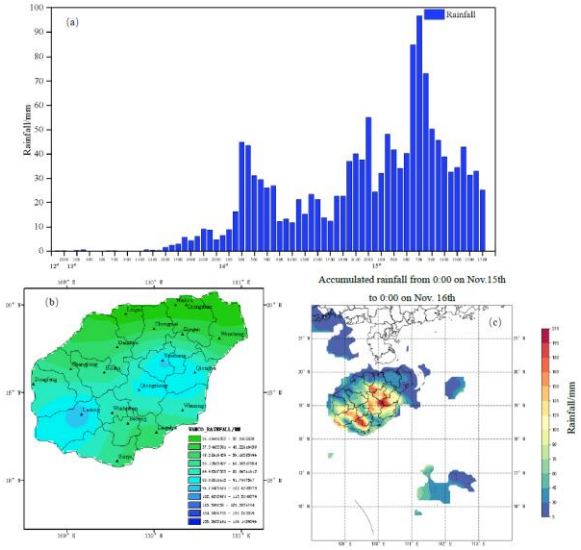

Figure 4: Spatial and temporal distribution of the measured rainfall of typhoon "VAMCO" (2022)(a~b) and the distribution of the accumulated rainfall from 00:00 on November 14 to 00:00 on November 16 (c)

It can be seen that Sansha City, Hainan Province is always subject to stronger wind and rain. When the typhoon is moving from east to west, the more northerly the typhoon path is, the more area of Hainan Island is affected by the wind and rain brought by the typhoon, especially the eastern and southern parts.

4 Analysis of Characteristics of Atmospheric Circulation during Multi-Typhoon

4.1 Analysis of Weather Situations

Taking the circulation situation of typhoon "NANGKA", "SAUDEL" and "VAMCO" as an example. Figure 5a1-a3 shows that there is cold air southward constantly in the 500hpa potential height field, in the process of the Mongolian cyclone strongly development eastward. At this moment, the vice high also strengthens the westward expansion, providing guidance airflow to the

typhoon's movement, and the typhoon moves westward. In combination with the wind field of 925hpa, the dry and cold air from the north to the south and the typhoon bring warm and humid airflow just meet in Hainan Province and the western part of Guangdong, which occurred a fierce collision and produced a strong storm process. With the dry and cold air heading south, the relative humidity is low in most of China by November, which is basically below 60% (Figure 5a3), but the relative humidity in Hainan Province is still above 70%. The area with high water vapor flux is basically located in Hainan Province and western Guangdong Province. There is a large amount of water vapor convergence when a typhoon lands or approaches Hainan Province (Figure 5b1-b2). It shows that there is a large amount of water vapor convergence in the horizontal direction in this area. The water vapor content is sufficient in the process of precipitation, and the water vapor flux in the precipitation area is large. The vertical latitudinal profile with the vertical velocity of typhoon center position can be seen (Figure 5c1-c2), which basically corresponds to the longitude span of Hainan Province near 108-111 ℃. Below 300hpa, there are negative velocity areas and the absolute value is large, which shows that the airflow has strong upward movement and the upward velocity reaches -0.8pa/s. The position of precipitation also conforms to each other with the vertical upward location.

It can be seen that the overall circulation situation in October-November is essentially a continuous southward movement of cold air. Under the guidance of the partial southeasterly airflow at the edge of the substratum, water vapor is irradiated in Hainan Province and the western part of Guangdong. The corresponding vertical velocity of the whole layer is basically in the negative zone, which means that a constant stream of water vapor gathers in this area and the value is on the higher side.

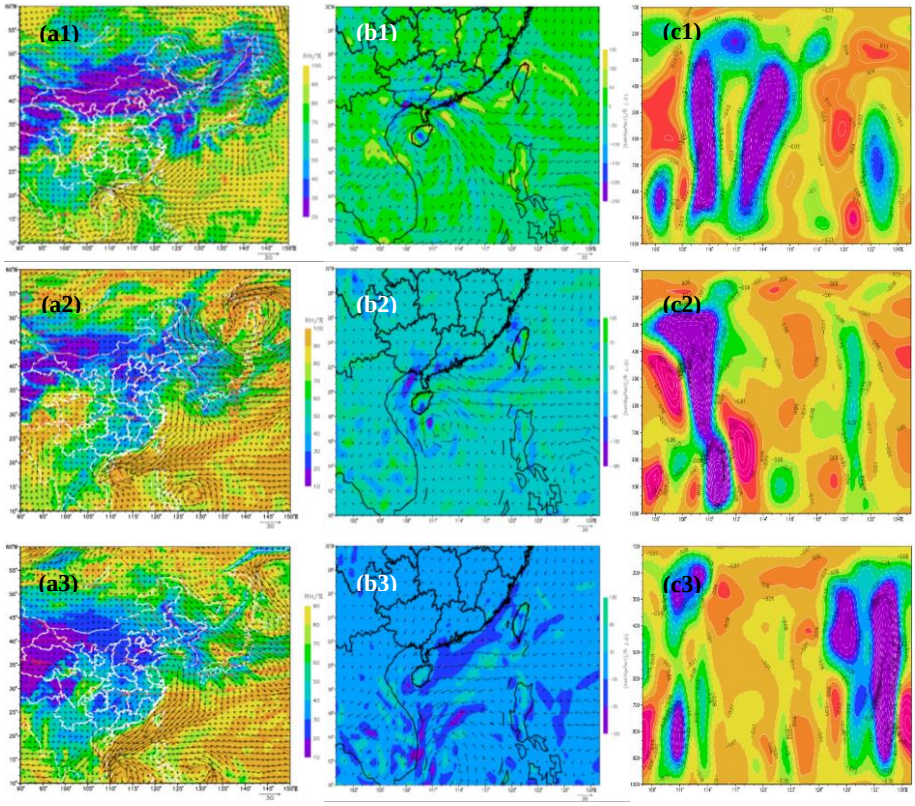

Figure 5: 925hpa wind field (arrow), relative humidity (shaded) superimposed on 500hpa geopotential height field (contour line) (a1-a3), 850hpa wind field (arrow)and vapor flux divergence (shaded) (b1-b3), and vertical velocity distribution (c1-c3) at 20:00 on October 13, 20:00 on October 24, and 14:00 on November 9

4.2 Sea Surface Temperature Field Features

When the sea temperature reaches above 26~27℃, it is conducive to the formation of typhoon[37-38]. Chan et al[39] showed that the intensity of tropical cyclones responds to SST changes almost contemporaneously. The reason why the super typhoon "SAOMAI" produced more water vapor and energy in 2008 is that the high SSTs contributed to the strengthening of the low-level cyclonic circulation and upper-level dispersion outflow in the typhoon area, which caused a constant water vapor amplitude rise in the low-level and a large amount of latent heat of condensation to be released, making the typhoon continue to develop and strengthen[40]. The super typhoon "RAMMASUN" in 2014 was also the result of the SST above 30 ℃ in the region where it was generated and the region where it will pass in the future, which made its lower atmosphere get more warm and wet air and provided adequate power for the development and strengthening of "RAMMASUN"[41]. Thus, it can be seen that SST has a very significant influence on the generation and development of typhoons[42].

Combined with the sea surface temperature anomaly in October 2020 (Figure 6a), there is a large-scale pleion in the equatorial western Pacific (west of 180 ℃), whereas the sea surface temperature pleion in November decreases compared with October, with a negative pleion in part of the South China Sea from the Gulf of Tonkin along the coast of the South China Peninsula, but there is still a large-scale sea surface temperature pleion on the ocean surface to the east of the Philippines, which may also be one of the reasons why typhoons are still generated in November. The global SST Convergence Actual Analysis Product (CODAS) (Figure 6c~d) shows that the monthly average global SST in October is higher in the western equatorial Pacific, that is, the temperature of surface of the ocean to the east of the Philippines is higher. This is generally consistent with the performance of sea surface temperature anomaly in October. The range of monthly average global sea surface temperature in November is narrower than that in October, however, higher sea surface temperature can still be seen in the equatorial western Pacific. All in all, whether in terms of long time horizon or in terms of convergence realities, the higher sea surface temperature in the western equatorial Pacific provides environmental conditions for typhoon generation.

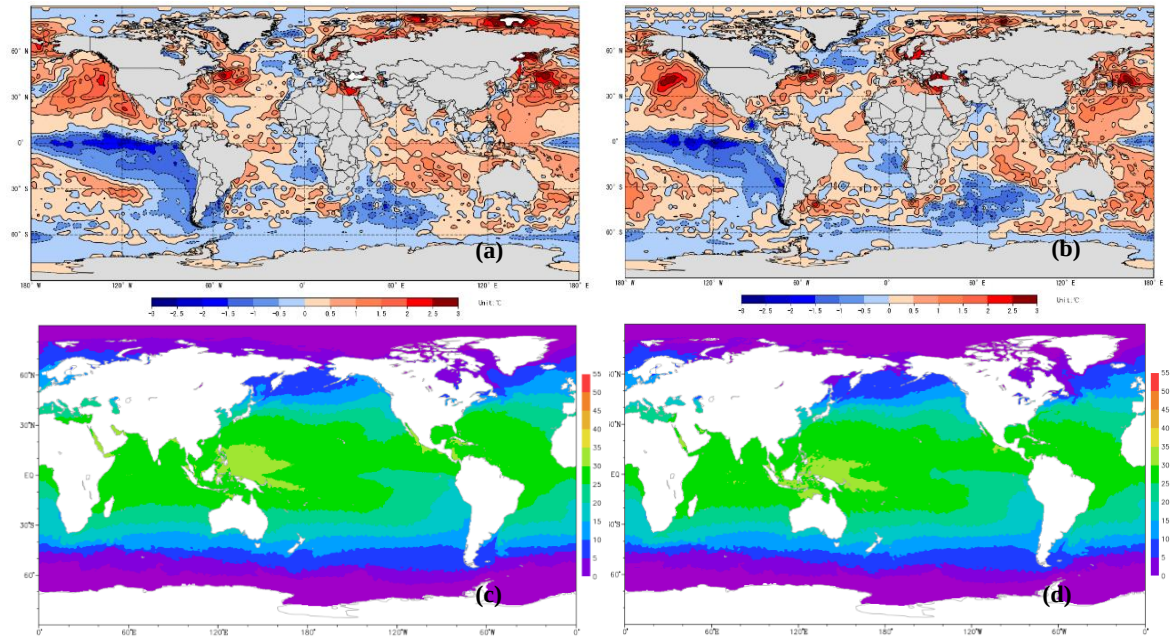

Figure 6: Sea Surface Temperature Anomaly in October (a) and November (b) 2020, global SST integration live products in October (a) and November (b) 2020 (unit: ℃)

4.3 Outgoing Long Wave Radiation (OLR) Distribution Features

The value of Outgoing Long wave Radiation (OLR) is mainly determined by the temperature of the land surface and the status of clouds, which is the temperature of cloud tops. Nevertheless, since the spatial and temporal distribution of temperature in the land surface of the tropics is less varied, the OLR depends mainly on the cloud situation, that is, it can be a reflection of the main convective and sinking zones in the tropics, and its low value zone is the main convective, cloudy and rainy zone. The high value zone of the OLR is in the trade wind zone or in the sinking zones controlled by the subtropical high pressure vice versa. Therefore, OLR is an indispensable element for studying and forecasting low-latitude general circulation and systems, and is useful for strengthening the ITCZ and promoting typhoon generation and development[43-46].

In terms of the distribution of the OLR pitch level in October and November 2020, there is a negative OLR pitch level area in October near the western Pacific Ocean and the South China Sea (Figure 7a), which indicates that there is a large-scale severe convection activity in this area with a central pitch level value of -75 W/M^2 or more.

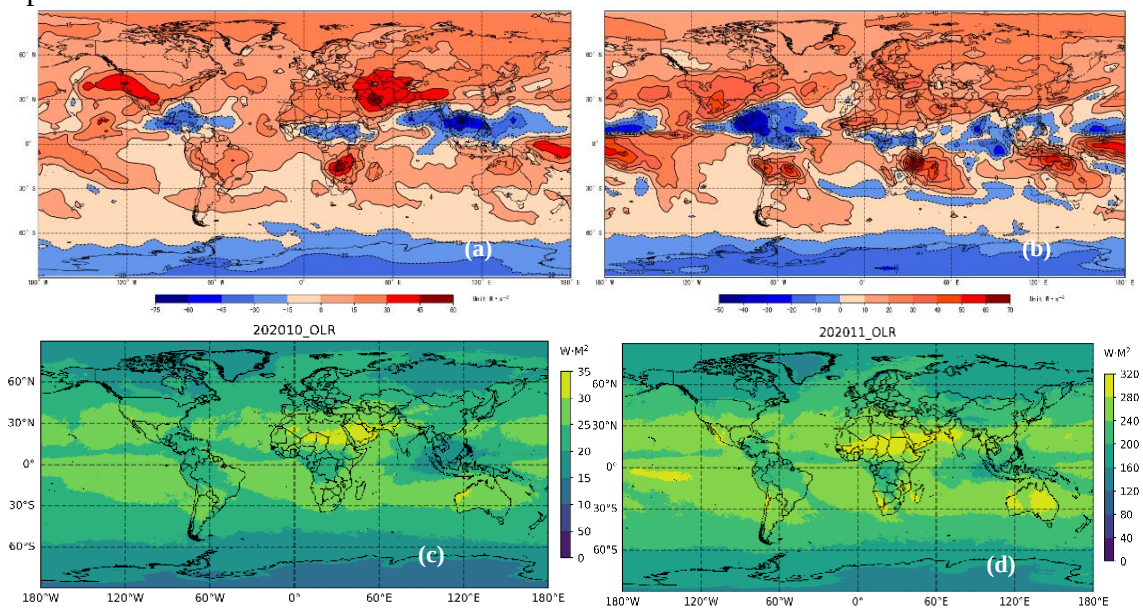

Figure 7: Outgoing Long wave Radiation (OLR) anomaly field in October (a) and November (b) 2020, global FY-3D emitting long wave radiation products in October (c) and November (d) 2020 (unit: W/M2)

On the contrary, the pleion is dominant on its eastern side, which suggests that sinking currents are dominant here. Compared to a negative distance level area in October, the scope of the negative distance level area near the western Pacific and South China Sea is reduced in November(Figure 7b), but there are still upward convective activities, and the central value of distance level reaches -20 W/M^2 or more. In combination with the monthly products of FY-3D radioactive long wave radiation in October, there is a zone of large OLR values in the western Pacific Ocean and near the South China Sea (Figure 7c), whose central value reaches 200 W/M2 or more, which indicates there is extensive strong convective activity in this area. Moving further east, the OLR values decrease slightly, with the low values ranging from 150 to 200 W/M^2. In contrast, the range of OLR large value areas in the western Pacific and South China Sea in November is reduced (Figure 7d), but convective activities still exist. In conjunction with the actual observations, it can also be seen that multi-typhoon primaries are mainly concentrated in the 5-20 °N, 110-150 °E regional range in October and November 2020. In addition to the impact of the interaction between typhoons and

cold air from the north south, there is a wide range of convective activities occurring in the western Pacific Ocean, the South China Sea waters to the South Central Peninsula.

5. Conclusion and Discussion

Oct-Nov 2020 typhoon generation in the South China Sea and the western Pacific sea concentrated in the Hainan Province, causing a significant impact on the characteristics of its atmospheric circulation conditions. This paper has made a preliminary analysis of its atmospheric circulation situation and its possible generation causes, and the following conclusions were obtained by using various data independently developed by China.

(1) In 2020, although the number of typhoons generated and landed in the northwest Pacific Ocean and the South China Sea waters of China is relatively less than that of previous years, and even no typhoons generated or landed in the South China Sea waters and the western Pacific Ocean in July. Although only one typhoon made landfall in China, the eight typhoons generated in succession within two months still brought relatively strong gale and rainstorm processes to Hainan Province during the period of October-November.

(2) From October to November 2020, the overall circulation situation is generally characterized by cold air continuously moving southward. The typhoon is guided by the partial southeasterly airflow at the edge of the substratum, and the water vapor is converging in Hainan Province and western Guangdong Province, which corresponds to a zone of negative vertical velocity of the whole layer, which indicates that a constant source of water vapor is accumulating in this region and the value is large.

(3) There was a large pleion in the western equatorial Pacific (west of 180 ℃) in October 2020, which may be one of the reasons for the continuous generation of typhoons in the South China Sea and the western Pacific in October. Even though the range of SST pleion in November is reduced compared with that in October, there is still a wide range of SST pleion on the ocean surface to the east of the Philippines, which may also be one of the reasons why typhoons still generated in the western Pacific Ocean in November.

(4) In October 2020, there is a negative anomaly area of OLR in the western Pacific and near the South China Sea, which means that there is a large-scale strong convective activity in this area. Compared with the negative anomaly area in October, the negative anomaly area has been reduced in scope near the western Pacific and the South China Sea in November, but there is still upward convective activity. Combining with the actual observations, it can also be seen that the areas of convective activity, which are also the primordial sites of typhoons, which are mainly concentrated within the region of 5-20 ℃N and 110-150 ℃E.

(5) Multi-source fusion data products and CRA-40 reanalysis data products independently developed by China can well reflect the general circulation situation and causes of multiple typhoons.

This paper explores the characteristics of multi-typhoon frequency, the atmospheric circulation situation and its influence in October-November 2020 in China, from which some preliminary conclusions are obtained. However, the specific evolution and generation characteristics of each typhoon still need to be investigated in more details in the future.

Acknowledgement

This work was funded by the National Key R&D Program, Grant number 2018YFC1506601. We acknowledge the critical comments from anonymous reviewers and editor.

References

[1] Defu Liu, Fengqing Wang. Typhoon/Hurricane/Tropical Cyclone Disasters: Prediction, Prevention and Mitigation. Journal of Geoscience and Environment Protection, 2019, 7, 26-36.

[2] Kennedy A B , Mori N , Zhang Y , et al. Observations and Modeling of Coastal Boulder Transport and Loading During Super Typhoon Haiyan. Coastal Engineering Journal, 2016, 58 (1): 1640004.1-1640004.25.

[3] Rebecca S, Stephanie T, Samantha K, et al. Preliminary Assessment of Hurricane Harvey Exposures and Mental Health Impact. International Journal of Environmental Research & Public Health, 2018, 15 (5): 974.

[4] Chen Lianshou, Ding Yihui. Generality of the Western Pacific Typhoon. Beijing: Science Press, 1979, 1.

[5] WANG Chengwei, QI Duo, XU Yue, ZHANG Libao, HU Zhongming, ZHOU Ying, WANG Qingyu. Analysis of Rainstorm Induced by Interaction between Typhoon Chan-hom (2015) and Cold Air in Northeast China. Plateau Meteorology, 2017, 36 (5): 1257-1266.

[6] Chen Lianshou, Xu Yinglong. Review of Typhoon Very Heavy Rainfall in China. Meteorological and Environmental Sciences, 2017, 40 (1): 3-10.

[7] LI Qiang, LIU De, WANG Zhong, LIAO Jun, ZHAI Danhua. Case Analysis on Heavy Rainstorm Caused Southwest Vortex under the Influence of Long-Distance Typhoon. Plateau Meteorology, 2013, 32 (3): 718-727.

[8] Lei Xiaotu. Progress of Unmanned Aerial Vehicles and Their Application to Detection of Typhoon Cyclone. Advances in Earth Science, 2015, 30 (2): 276-283.

[9] HUANG Jing, LI Hai-ying, WU Jia-hao. Wind Field Structure of the Tropical Cyclone Pabuk by Means of Wind Profiler Data. Guangdong Meteorology, 2009, 31 (1): 5-8.

[10] Liang Hongsheng, Xie Jianqun. Causes of Heavy Rainfall in Eastern Guangdong Induced by Tropical Storm "Lianhua". Journal of Meteorological Research and Application, 2009, 30 (a02): 102-104.

[11] Meng Zhaozhen, Chen Jian, Han Shenyou, Lai Zhenquan, Zhai Liping, Lin Kaiping. Characteristic Analysis on Rainstorms of Typhoon Remnant Vortexes in Guangxi. Journal of Meteorological Research and Application, 2017, 38 (1): 20-25.

[12] Zheng Fengqin, Wang Shengfan, Zhao Jinbiao, et al. Analysis on the characteristics of typhoon Extreme Precipitation and the anomaly ofenvironmental parameters in Guangxi. Journal of Meteorological Research and Application, 2021, 42(4): 07-13.

[13] Zhou Guanbo, Ran Lingkun, Gao Shouting, et al. High-resolution numerical simulation and diagnostic analysis of dynamic structure of typhoon "Morakot". meteorology, 2015, 41 (6): 727-737.

[14] Tang Yushuang. Analysis of mesoscale characteristics of radar rain belt: Typhoon "Morakot" (2009). Taoyuan: National Central University of Taiwan Province, China, 2010.

[15] Wang Xiao, Yu Hui, Bao Xuyi, et al. Analysis on extreme characteristics of the precipitation brought by typhoon "Titow" (1323). Journal of the Meteorological Sciences, 2017, 37 (4): 514-521.

[16] Chen Yan, Wu Yu, Wang Tianwei. Analysis of the Intensification Causes of Super Typhoon "Rammasun" (1409) in the Coastal Waters. Chinese journal of tropical agriculture, 2020, 40 (1): 120-126.

[17] Chen Hong. The Influence of Typhoon on the Economy of Guangdong Province —— Based on CGE Model. NanJing university of information science &technology, 2021.

[18] Dong Meiying, Chen Feng, Qiu Jinjing, et al. 2021. Impact of Spectral Nudging Technique Driven with ECMWF Data on the Fine Numerical Prediction of Super Typhoon Lekima (2019) in Zhejiang Province . Chinese Journal of Atmospheric Sciences (in Chinese), 45 (5): 1071−1086.

[19] Ding Yihui, Fan Huijun, Xue Qiufang, Chen Guixiang. A preliminary study on the simultaneous development of multiple typhoons in the tropical zone. Scientia Atmosphrica Sinica, 1977 (2): 89-98.

[20] ZHANG Chunyan, WANG Li, SUN Mingming, Zhang Jianhai. Tentative analysis on multi-typhoon characteristics and atmospheric circulation background in the midsummer of 2012. Torrential Rain and Disasters, 2012, 31 (4): 298-305.

[21] Yang Zu-fang, He Shi-xiu. A Circulation Pattern Favorable for the Frequent Occurrence of Typhoon over Southwest Pacific. Scientia Atmospherica Sinica, 1982, 6 (3): 293-300.

[22] William M. Gray, Tropical cyclone genesis in the western North Pacific. JMeteor Soc Japan, 1977, 55 (4): 465-482.

[23] Xu Jinjing, Li Hongtu. Climatic analysis of typhoon activities in Fujian in 1999. Marine Forecasts, 2000, 17 (4): 28-33.

[24] Peng Benxian. Analysis of Typhoon in South China Sea in October 1983. Journal of Guangxi Meteorology, 1985 (04): 6-9.

[25] Liu Na, Chou Shilian, Duan Mingguo, Wang Zhiyu. Analysis of circulation characteristics of multiple typhoons in Jilin Province in 2018 . Meteorological Disaster Prevention, 2021, 28 (1): 1-5.

[26] Xie, P. P., and A. Y. Xiong, A conceptual model for constructing high-resolution gauge-satellite merged

precipitation analyses, Journal of Geophysical Research, 2011,116, doi: 10.1029/ 2011JD016118.
[27] Qingyun Duan, Newsah K. Ajami, Xiaogang Gao, Soroosh Sorooshian. 2007. Multi-model ensemble hydrologic prediction using Bayesian model averaging. Elsevier, Adv. Water Resource, 30: 1371-1386.
[28] Pan Yang, Shen Yan, Yu Jingjing, Xiong Anyuan. An Experiment of High-Resolution Gauge-Radar-Satellite Combined Precipitation Retrieval Based on the Bayesian Merging Method. Acta Meteorologica Sinica, 2015, 73 (1): 177-186.
[29] Pan Yang, Shen Yan, Yu Jingjing, Zhao Ping. Analysis of the Combined Gauge-Satellite Hourly Precipitation over China Based on the OI Technique. Acta Meteorologica Sinica, 2012, 70 (6): 1381-1389.
[30] Yu Jingjing, Shen Yan, Pan Yang, Zhao Ping, Zhou Zijiang. Improvement of Satellite-based Precipitation Estimates over China Based on Probability Density Function Matching Method. Journal of Application Meteorological Science, 2013, 24 (5): 544-553.
[31] Y Shen, P Zhao, Y Pan, J Yu. 2014. A high spatiotemporal gauge-satellite merged precipitation analysis over China. J Geophys Res, 119, doi:10.1002/2013JD020686.
*[32] X. Liang, L. P. Jiang, Y. Pan, Chunxiang Shi, 2020: A 10-yr global land surface reanalysis interim dataset (CRA-Interim/Land): Implementation and preliminary evaluation. J. Meteor. Res., **34**, 101–116. doi:10.1007/s13351-020-9083-0.*
*[33] B. Zhao, B. Zhang, C. X. Shi, J. W. Shi, 2019: Comparison of the global energy cycle between Chinese reanalysis interim and ECMWF reanalysis. J. Meteor. Res., **33**, 563–575. doi: 10.1007/s13351-019-8129-7.*
*[34] C. X. Li, T. B. Zhao, C. X. Shi, Z. Q. Liu, 2020: Evaluation of daily precipitation product in China from the CMA global atmospheric interim reanalysis. J. Meteor. Res., **34**, 117–136. doi: 10.1007/s13351-020-8196-9.*
[35] Zhao D, Zhang L, Zhou T, Liu J. Contributions of Local and Remote Atmospheric Moisture Fluxes to East China Precipitation Estimated from CRA-40 Reanalysis. Journal of Meteorological Research, 2021.
[36] Y. B. Zhang. Quick glance at the 2020 China Climate Bulletin. China Meteorological News, 2021-02-10 (003).
[37] Charles R. Holliday, Aylmer H. Thompson. Climatological characteristics of rapidly intensifying typhoons. Monthly Weather Review, 1979, 107 (8): 1022-1034.
[38] SHI Shun-ji, YU Jin-hua, ZHENG Li-xin. An Analysis of the Environment Effect on Super Typhoon Sepat (0709). Journal of Oceanography in Taiwan Strait, 2009, 28 (01): 135-141.
[39] Chan J.C.L., Shay L K., Duan Y H. Tropical cyclone intensity change from a simple ocean-atmosphere coupled model. Journal of the Atmospheric Sciences, 2001, 58 (2): 154-172.
[40] Xue Gengyuan, Zhang Jianhai, Chen Hongmei, Yu Hai. Analysis on Causes of Strengthening of Super Strong Typhoon Saomai (0608) and Numerical Experiments of the Impact of SST on Its Intensity. Quaternary Sciences, 2007 (03): 311-321.
[41] CHEN Yan, WU Yu, WANG Tianwei. Analysis of the Intensification Causes of Super Typhoon "Rammasun"(1409) in the Coastal Waters. Chinese Journal of Tropical Agriculture, 2020, 040 (001):120-126.
[42] Kaplan J, Demaria M. Larger-scale characteristic of rapidly intensifying tropical cyclones in the north Atlantic basin. Wea Forecasting, 2003, 18 (6): 1093-1108.
[43] Xie An, Chen Longxun, Murakami. The Seasonal Characteristics and Interannual Variability of the Tropical Circulation Shown by the Earth's Outward Long-wave Radiation (OLR) Data. Acta Oceanologica Sinica, 1988 (01): 38-45.
[44] Xie An, Ye Qian. Relationship between OLR Low-frequency Oscillations and the Formation of Typhoon over the Western Pacific. Quarterly Journal of Application Meteorological, 1994 (02): 143-150.
[45] Jiang Shangcheng, Zhang Weidong. The Climatic Characteristics of the Subtropical High Pressure over the Northern Pacific Revealed by OLR. Geographical Research, 1994 (02): 27-33.
[46] DUAN Li, JIANG Shang-cheng. Use of Monthly Mean OLR Departure in Investigating the Landing of TC and Its Impact on the Southern China in Summer. Journal of Tropical Meteorology, 2001 (03): 258-264.